

Spectroscopy of light nuclei with Skyrme-type interactions

V B KAMBLE* and S B KHADKIKAR

Physical Research Laboratory, Ahmedabad 380 009

*Present Address: Vikram A. Sarabhai Community Science Centre,
Ahmedabad 380 009

MS received 18 November 1978; revised 19 September 1979

Abstract. Deformed Hartree-Fock calculations are performed for some light nuclei in a large configuration space consisting of first four major shells. The interaction employed is the modified Skyrme interaction in which the deformed density is replaced by the band averaged scalar density that makes the Hamiltonian rotationally invariant rendering the spectroscopic calculations feasible. It is shown that the introduction of density dependence spreads out the energy spectra and that the Skyrme variant SIV which has a weak density dependence gives best overall agreement for energy spectra and the available data for the electromagnetic properties of the nuclei studied. It is found that the maximum contribution to the energy of any state in the low lying spectrum comes from the s -state attractive and s -state repulsive parts of the Skyrme interaction. It is also shown that when two-body density dependent version of Skyrme interaction is used, the Koopmans theorem no longer holds.

Keywords. Skyrme interaction; density dependent Hartree-Fock; band averaged density; projected spectra; electromagnetic properties; ^8Be ; ^{12}C ; ^{16}O ; ^{20}Ne .

1. Introduction

The density dependence of the effective interaction or G -matrix arises naturally due to the exclusion principle. The effective interaction depends very much on the presence of the other nucleons since they prevent the two interacting nucleons from scattering into the states which they occupy. This makes G a very complicated function. Therefore a simplifying assumption made for G is that the effect of other nucleons is accounted for by representing G as a density dependent function of the two nucleon co-ordinates. The Skyrme interaction is a simple parametrisation of the G -matrix and is purely a phenomenological fit to the G -matrix with zero-range forces and a three-body force simulating a two-body density-dependent force.

Recently there have been many attempts to use phenomenological forces of the type given by Skyrme (1956, 1959) or realistic density-dependent forces (Vautherin and Brink 1972; Vautherin 1973; Friar and Negele 1975; Beiner *et al* 1975; Zofka and Ripka 1971, etc.), to reproduce binding energies, sizes and other intrinsic properties of the nuclei. Although the Skyrme interaction is characterised by only a few parameters, many different sets of these parameters (Vautherin and Brink 1972, Beiner *et al* 1975) have been obtained which more or less fit the binding energies and rms radii for nuclei all over the periodic table.

In spite of the phenomenal success achieved with Skyrme interactions in reproducing bulk properties of nuclei, there have been few efforts in calculating spectroscopic properties such as energy spectra (Bertsch and Tsai 1975; Passler and Mosel 1976; Caurier and Grammaticos 1977; Khadkikar and Kamble 1976), transition rates, etc.

using such interactions. It would be interesting to see if one can obtain information about the parameters of the Skyrme interaction by calculating spectroscopic properties and see if certain spectroscopic properties are sensitive to some of the parameters of the Skyrme force. The spectroscopic calculations would provide additional criteria to choose among the several variants of the Skyrme interaction. This is precisely what motivated us to carry out spectroscopic calculations with the Skyrme-type interactions. The three-body force simulating density-dependence in the Skyrme interaction has the unpleasant feature of overbinding odd-mass and odd-odd nuclei and producing unstable spin-aligned Hartree-Fock (HF) ground states in nuclear matter and even-even nuclei (Chang 1975; Passler 1976). Thus a two-body density-dependent interaction is preferred to a three-body force for maintaining the time-reversal invariance of the lowest HF states. On the other hand, the equivalent two-body density-dependent force in HF approximation is rotationally non-invariant for deformed nuclei, thus rendering it unsuitable for rigorous spectroscopic calculations requiring good angular momentum eigenstates, though this force has been used (Passler and Mosel 1976) in self-consistent cranking model. In this paper, we employ the modified version of the Skyrme interaction (Khadkikar and Kamble 1976) which enables us to perform spectroscopic calculations by employing a scalar density-dependence averaged over the whole band of states contained in the variational intrinsic state. Such an interaction would be equivalent to the usual Skyrme force in spherically-symmetric nuclei thus maintaining the agreement for bulk properties obtained all over the periodic table. We performed projected HF calculations with several Skyrme variants. We shall show that this procedure leads to energy spectra in excellent agreement with experiment with a Skyrme variant having weak density-dependence, the calculations being performed in the framework of projected multi-major shell HF formalism. We shall also show how each term in the Skyrme force contributes to the energy spectra.

In § 2, we shall discuss the Skyrme interaction and the modification proposed so that the spectroscopic calculations are made completely feasible. In § 3, we shall outline the HF formalism employing density-dependent interactions. We shall discuss the single particle separation energies and the suitability of the Skyrme interaction for spectroscopic calculations and present the HF results for the bulk properties of some even-even time-reversal invariant nuclei (for the sake of simplicity). In § 4, we shall study the HF projected spectra for the nuclei studied and discuss how individual parts of the Skyrme interaction contribute to the energy spectra. In § 5, the electromagnetic properties obtained with the good angular momentum projected states are discussed and compared with the experiment. In § 6, the main conclusions are summarised.

2. Skyrme interaction and the definition of the band averaged density

2.1. Skyrme interaction

The Skyrme interaction has a two-body part v_{12} and a three-body part V_{123}

$$V = v_{12} + V_{123}, \quad (1)$$

Skyrme used a short range expansion of two-body interaction. For Hartree-Fock calculations only low-momentum matrix elements ($\mathbf{k}, \mathbf{k}' \leq 2 K_F$) are required where \mathbf{k} and \mathbf{k}' are relative wave-vectors of the two nucleons. In the co-ordinate space, v_{12} can be written as

$$v_{12} = t_0(1 + \chi_0 P \sigma) \delta(\mathbf{r}_1 - \mathbf{r}_2) + \frac{1}{2} t_1 [\delta(\mathbf{r}_1 - \mathbf{r}_2) k'^2 + k^2 \delta(\mathbf{r}_1 - \mathbf{r}_2)] \\ + t_2 \mathbf{k}' \cdot \delta(\mathbf{r}_1 - \mathbf{r}_2) \mathbf{k} + iW(\sigma_1 + \sigma_2) \cdot \mathbf{k}' \times \delta(\mathbf{r}_1 - \mathbf{r}_2) \mathbf{k}. \quad (2a)$$

For the three-body force, Skyrme assumed a contact force,

$$V_{123} = t_3 \delta(\mathbf{r}_1 - \mathbf{r}_2) \delta(\mathbf{r}_2 - \mathbf{r}_3). \quad (2b)$$

The operator $\mathbf{k} = (\vec{\nabla}_1 - \vec{\nabla}_2)/2i$ acts on the right, while $\mathbf{k}' = -(\vec{\nabla}_1 - \vec{\nabla}_2)/2i$ acts on the left. It is easy to show that the matrix elements of the first two terms in (2a) correspond to s -wave interactions. The matrix elements of the other two terms correspond to p -wave interactions. The last term is, in fact, the zero range limit of a two-body spin-orbit force (Bell and Skyrme 1956).

It was shown by Vautherin and Brink (1972) that in the HF calculations of even-even nuclei, the three-body term (equation (2b)), is equivalent to a two-body density-dependent interaction,

$$V_{12} = (t_3/6) (1 + P \sigma) \delta(\mathbf{r}_1 - \mathbf{r}_2) \rho \{(\mathbf{r}_1 + \mathbf{r}_2)/2\}. \quad (3)$$

This is the form of the interaction used in the present work. The density dependent two-body force in Skyrme interaction describes how the interaction between two nucleons gets modified due to the presence of other nucleons. This phenomenological representation of G -matrix includes the effects of short range correlations particularly through the density-dependent term. The contribution to total energy due to the two-body density-dependent term does not vanish for spin-aligned solutions unlike the three-body contact force and thus contributes to saturation. Two-body density-dependent force is therefore always preferred to three-body contact force.

2.2. Definition of the band averaged density

The density appearing in the two-body density-dependent part of the Skyrme interaction needs to be evaluated at the centre-of-mass of two interacting nucleons. However, for a contact force, such as Skyrme interaction this coincides with density at the position of either of the two interacting nucleons. The density $\rho(\mathbf{r})$ is defined as,

$$\rho(\mathbf{r}) = \sum_{i=1}^A \langle \mathbf{r} | \phi_i \rangle \langle \phi_i | \mathbf{r} \rangle. \quad (4)$$

The density $\rho(\mathbf{r})$ for an axially deformed time-reversal invariant even-even nucleus can be expanded in terms of its multipole components as follows:

$$\rho(\mathbf{r}) = \sum_L \rho_L(\mathbf{r}), \quad L = 0, 2, 4, \dots \quad (5)$$

It is easy to see that the scalar part of density $\rho_0(\mathbf{r})$ can be expressed as the average of scalar densities of the states projected onto the space of good angular momentum:

$$\rho_0(\mathbf{r}) = \sum_J |a_J|^2 \rho_0^J(\mathbf{r}), \quad (6)$$

where
$$\rho_0^J(\mathbf{r}) = \frac{1}{2J+1} \sum_M \langle J M | \rho_{\text{op}} | J M \rangle,$$

and
$$\rho_{\text{op}} = \sum_{i=1}^A \delta(\mathbf{r}_i - \mathbf{r}).$$

Here $|a_J|^2$ is the probability of the state with angular momentum J contained in the deformed intrinsic state.

We suggest a modification in the interaction (Khadkikar and Kamble 1976) such that the deformed density $\rho(\mathbf{r})$ is replaced by the 'band averaged' scalar density $\rho_0(\mathbf{r})$. V_{12} is then replaced by V'_{12} where,

$$V'_{12} = (t_3/6) (1 + P\sigma) \delta(\mathbf{r}_1 - \mathbf{r}_2) \rho_0 \{(\mathbf{r}_1 + \mathbf{r}_2)/2\}. \quad (7)$$

The interaction V'_{12} would retain the rotational invariance and at the same time would not disturb the agreement for the bulk properties for spherical nuclei. It is straightforward to obtain the expression for $\rho_0(\mathbf{r})$ to be used in the HF calculations.

$$\rho(\mathbf{r}) = \sum_{i=1}^A \langle \mathbf{r} | \phi_i \rangle \langle \phi_i | \mathbf{r} \rangle, \quad (8a)$$

which when expanded in terms of the basis states $|n_a l_a j_a m_a\rangle$ assuming axial symmetry and the non-mixing of proton and neutron orbitals,

$$\rho(\mathbf{r}) = \sum_{i=1}^A \sum_{\alpha\beta} c_{\alpha}^{i*} c_{\beta}^i \langle \mathbf{r} | \beta, m_i \tau_i \rangle \langle \alpha, m_i \tau_i | \mathbf{r} \rangle, \quad (8b)$$

where $\alpha = n_a l_a j_a$ and the c 's are the expansion coefficients.

Equation (8b) can be written as,

$$\begin{aligned} \rho(\mathbf{r}) &= \sum_{i=1}^A \sum_{\alpha\beta} c_{\alpha}^{i*} c_{\beta}^i (-1)^{j_{\alpha} - m_i} \\ &\times \sum_J c \begin{pmatrix} j_{\alpha} & j_{\beta} & J \\ -m_i & m_i & 0 \end{pmatrix} \langle \mathbf{r} | \Psi^J(\alpha, \beta, \tau_i) \rangle \end{aligned} \quad (8c)$$

where $\langle \mathbf{r} | \Psi^J(\alpha, \beta, \tau_i) \rangle$

$$\begin{aligned} &\equiv \sum_{m_{\alpha} m_{\beta}} (-1)^{j_{\alpha} - m_{\alpha}} c \begin{pmatrix} j_{\alpha} & j_{\beta} & J \\ -m_{\alpha} & m_{\beta} & M \end{pmatrix} \\ &\times \langle \mathbf{r} | \beta, m_{\beta}, \tau_i \rangle \langle \alpha, m_{\alpha}, \tau_i | \mathbf{r} \rangle. \end{aligned}$$

Zeroth multipole of the density can be extracted by setting $J = 0$. It is then trivial to show that (8c) reduces to

$$\rho_0(\mathbf{r}) = \sum_{i=1}^A \sum_{\alpha\beta} c_{n_\alpha l_\alpha j_\alpha}^{i*} c_{n_\beta l_\beta j_\beta}^i \times \left(\frac{1}{2J_\alpha + 1} \right) \sum_{m_\alpha} \langle \mathbf{r} | n_\beta l_\beta j_\beta m_\alpha, \tau_i \rangle \langle n_\alpha l_\alpha j_\alpha m_\alpha, \tau_i | \mathbf{r} \rangle. \quad (9)$$

This is then the expression to be used in the HF calculations for the 'band averaged' scalar density. Introduction of this band-averaged scalar density now makes the Hamiltonian rotationally invariant and the spectroscopic calculations are made completely feasible and the difficulties caused by the three-body contact force overcome.

3. Density dependent Skyrme interaction in HF formalism

3.1. Density dependence in HF theory

In this section we shall briefly outline the HF formalism with density-dependent Skyrme forces. We shall assume axial symmetry and hence the deformed orbital $|i\rangle$ can be expanded as:

$$|i\rangle = \sum_a c_a^i |a, m_i, \tau_i\rangle,$$

with $a = n_\alpha l_\alpha j_\alpha$. (10)

In the deformed basis, the nuclear Hamiltonian using the two-body band averaged scalar density-dependent Skyrme interaction V'_{12} can be written as:

$$H = \sum_{ij} \langle i | t | j \rangle a_i^\dagger a_j + \frac{1}{2} \sum_{ijkl} \langle ik | v_{12} + V'_{12} | jl \rangle a_i^\dagger a_k^\dagger a_l a_j, \quad (11)$$

v_{12} denotes all the terms of the Skyrme interaction which are independent of density. When it does not cause confusion, we shall drop the quantum numbers m_i and τ_i . Denoting by $|\phi\rangle$ the A particle state,

$$|\phi\rangle = \prod_{i=1}^A a_i^\dagger |0\rangle, \quad (12)$$

we have the total energy for the nucleus with A nucleons

$$E = \langle \phi | H | \phi \rangle = \sum_{i=1}^A \langle i | t | i \rangle + \frac{1}{2} \sum_{ij}^A \langle ij | \tilde{v}_{12} + \tilde{V}'_{12} | ij \rangle, \quad (13)$$

where tilde denotes the antisymmetrised matrix element.

The HF approximation requires that for all α s,

$$\frac{\partial}{\partial c_a^{i*}} [\langle \phi | H | \phi \rangle - \sum_{i=1}^A \epsilon_i \sum_a c_a^{i*} c_a^i] = 0,$$

$$\begin{aligned} \text{i.e.} \quad \frac{\partial}{\partial c_a^{i*}} & \left[\sum_{i=1}^A \langle i | t | i \rangle + \sum_{ij}^A \langle ij | \tilde{v}_{12} + \tilde{V}'_{12} | ij \rangle \right. \\ & \left. - \sum_{i=1}^A \epsilon_i \sum_a c_a^{i*} c_a^i \right] = 0. \end{aligned} \quad (14)$$

Here ϵ_i are the Lagrangian parameters. Equation (14) leads us to the following set of equations:

$$\sum_{\beta} \langle \alpha | h | \beta \rangle c_{\beta}^i = c_{\alpha}^i \epsilon_i, \quad (15a)$$

$$\begin{aligned} \langle \alpha | h | \beta \rangle & = \langle \alpha | p^2/2m | \beta \rangle \\ & + \sum_{\text{occ}}^A \sum_{\gamma\delta} \langle \alpha \gamma | \tilde{v}_{12} + \tilde{V}'_{12} | \beta \delta \rangle c_{\gamma}^{i*} c_{\delta}^i \\ & + (t_3/4) \langle \alpha | (\rho_p \rho_n)_0 | \beta \rangle. \end{aligned} \quad (15b)$$

Equations (15a) and (15b) are the HF equations to be solved self-consistently. The HF Hamiltonian h is defined through (15b). ρ_p (n) is the density of the protons (neutrons) and $(\rho_p \rho_n)_0$ is the zeroth multipole of the product $(\rho_p \rho_n)$. If we start with a spherical density, only the zeroth multipole of the product $(\rho_p \rho_n)$ contributes. It should be noted that the last term in (15b) arises purely out of the density dependence of the interaction.

The solution of (15a) and (15b) involves the problem of double self-consistency between the interaction matrix elements and the HF wave function. One starts with a trial wave function and calculates two-body scalar density matrix elements $\langle \alpha \gamma | \tilde{V}'_{12} | \beta \delta \rangle$ and the one-body density matrix elements $\langle \alpha | (\rho_p \rho_n)_0 | \beta \rangle$ and sets up the Hamiltonian matrix $\langle \alpha | h | \beta \rangle$. Its diagonalisation then gives a new set of eigen-values and eigen-functions. With this new wave function, again new two-body scalar density matrix elements are evaluated and the Hamiltonian matrix set-up and diagonalised. This procedure is continued until two successive wave functions and the sets of two-body matrix elements calculated are the same, i.e. when both interaction matrix elements and the HF solution are mutually self-consistent. It is clear from this procedure that the density-dependent HF calculations are an order of magnitude more difficult than the density independent ones.

3.2. Rearrangement energy

For density-independent forces, the total energy E of a nucleus can be expressed as

$$E = \frac{1}{2} \sum_{i=1}^A [\langle i | t | i \rangle + \epsilon_i]. \quad (16)$$

For Skyrme interaction, there is an additional term arising out of the density dependence of the interaction. The expression (16) is replaced by

$$E = \frac{1}{2} \sum_{i=1}^A [\langle i | t | i \rangle + \epsilon_i] + E_R, \quad (17)$$

where E_R is called the "rearrangement energy" and is given by

$$E_R = - (t_{3/8}) \sum_{i=1}^A \langle i | \rho_p \rho_n | i \rangle. \quad (18)$$

In our modified version of Skyrme interaction, only the zeroth multipole of the product $\rho_p \rho_n$ contributes and the expression becomes

$$E_R = - (t_{3/8}) \sum_{i=1}^A \langle i | (\rho_p \rho_n)_0 | i \rangle. \quad (19)$$

From the expression (19) for the rearrangement energy E_R , it can be seen that this quantity is always negative. In fact, this would be the case for any form of density dependence of interaction. Thus the total energy in density-dependent HF theory is always lower than the ordinary HF theory would lead us to expect from the given single-particle energy eigen values. For Skyrme force, the relation (16) is replaced by (17). The rearrangement energy term E_R which arises purely due to the density dependence of the interaction is then responsible in obtaining good agreement for binding energies of nuclei with experiment.

3.3. HF single particle energies and separation energies

We shall show in this section that if we consider the two-body density version of the force in Skyrme interaction rather than the three-body contact force, the Koopmans theorem (Koopmans 1934) no longer holds (Ripka 1969) assuming that the single-particle wave functions of the A and $A-1$ systems are identical. Koopmans theorem strictly holds when the three-body contact interaction is used as shown by Vautherin and Brink (1972).

It has been shown that the Koopmans theorem holds for density-independent two-body interaction only in the absence of centre-of-mass motion (c.m.m.) (Khadkikar and Kamble 1974). We shall not consider c.m.m. to make the discussion simple and concentrate only on the density-dependent part of the interaction.

The contribution $\epsilon_{(K)}^{(3)}$ to the HF single-particle energy $\epsilon_{(K)}$ for the orbital K from (15a) and (15b) for even-even time-reversal invariant nuclei due to the density-dependent part is given by

$$\epsilon_{(K)}^{(3)} = t_{3/4} \langle K | (\rho_0^A)^2 - (\rho_0^N)^2 | K \rangle, \quad (20)$$

considering K to be a neutron orbital. Here, ρ_0^A denotes the band-averaged density for the nucleus with A particles and ρ_0^N is the zeroth multipole of density of neutrons. This expression for HF single particle energies is identical with the one given by Vautherin and Brink (1972).

We shall give the expression for the contribution to separation energy due to the density-dependent part of Skyrme interaction, $\epsilon_{\text{sp}}^{(3)}(K)$, required to remove the nucleon from K th orbital assuming that the orbitals of the residual nucleus with $(A-1)$ nucleons do not change after sudden removal of the particle from the orbital K . Considering K to be the neutron orbital, it is easy to show that,

$$\epsilon_{\text{sp}}^{(3)}(K) = \epsilon_{(K)}^{(3)} - t_{3/4} \langle K | \rho_0^P \phi_K^* \phi_K | K \rangle. \quad (21)$$

We thus see that the separation energies differ from HF single-particle energies by an amount given by the second term in (21) and so the Koopmans theorem no longer holds when a two-body density-dependent interaction is used.

It should be noted that our expression for HF single-particle energies is identical with that of Vautherin and Brink and so with their separation energies since they use three-body contact force. Our expression for separation energies, however, is different. Three-body contact force and two-body density-dependent force are equivalent only for the even-even time-reversal invariant systems.

When c.m.m. is incorporated in HF calculations, the Koopmans theorem is not valid and the particle number A is to be treated as a number operator. We see that when the interaction itself depends on the particle number, the Koopmans theorem will not be valid. The total density of a system depends on the total number of particles A in the system and so the Koopmans theorem will not be valid for density-dependent interactions. The effect of the second term in (21) however is expected to be small, approximately by a factor $(1/A)$ and so $\epsilon_{\text{sp}}^{(3)}(K)$ and $\epsilon_{(K)}^{(3)}$ would be quite close especially when the number of nucleons is quite large. Hence single-particle energies would be quite close to the actual separation energies when density-dependent forces are used.

3.4. Suitability of Skyrme interaction for spectroscopic calculations

In this section we shall discuss the suitability of the Skyrme interaction for calculating the spectroscopic properties.

Sharp and Zamick (1973) calculated particle-particle two-body coupled pairing matrix elements using harmonic oscillator wave functions for the state $(0 f_{7/2})^2$ for the configuration in ^{42}Ca , important for the ground state energy spectrum. They report that this pairing matrix element for the Skyrme interaction gives a repulsive value for the $J = 0, T = 1$ and higher states. This would lead to an unphysical energy spectrum for ^{42}Ca . This suggests that one should check such pairing matrix elements for Skyrme interaction before calculating the spectroscopic properties.

We show that this difficulty can be overcome by a proper choice of the value of the oscillator parameter b . We studied the pairing matrix elements $(0 s_{1/2})^2, (0 p_{3/2})^2, (0 d_{5/2})^2$ and $(0 f_{7/2})^2$ for $J = 0, T = 1$ states as a function of the oscillator parameter b for the Skyrme variant SIV.

For the $(0 s_{1/2})^2$ and $(0 d_{5/2})^2$ matrix elements (m.e.), only t_0 and t_1 terms contribute while for $(0 p_{3/2})^2$ and $(0 f_{7/2})^2$ m.e., the t_2 and W terms also contribute a little. In either case, the most contribution to these matrix elements is due to t_0 and t_1 terms. Only t_0 and t_1 m.e. would decide whether the total m.e. would be attractive or repulsive.

We have plotted the pairing matrix elements ($J = 0, T = 1$) for $(-t_0)$ and t_1 terms for the $(0 s_{1/2})^2$ and $(0 d_{5/2})^2$ states and also the total m.e. (figures 1 and 2). The density-dependent part of the Skyrme interaction will not contribute to the matrix elements for $T = 1$ states due to antisymmetry requirements.

For the $(0 s_{1/2})^2 J = 0, T = 1$ m.e. (figure 1) one can see that the t_0 m.e. are always larger than the t_1 m.e. for any value of b and hence this m.e. shall always be attractive. Similar features are exhibited by $(0 p_{3/2})^2$ m.e.

The situation is rather interesting for the $(0 d_{5/2})^2$ m.e. (figure 2). For small values of b , the t_0 m.e. though attractive is numerically smaller than t_1 m.e. and the total

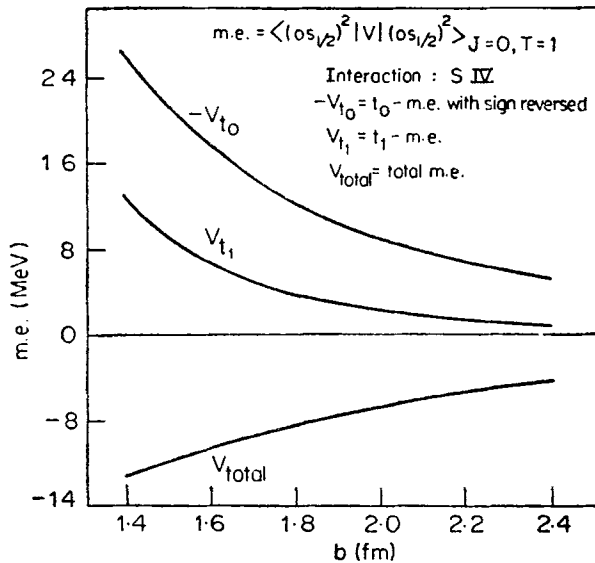


Figure 1. The matrix element $\langle (0 s_{1/2})^2 | V | (0 s_{1/2})^2 \rangle_{J=0, T=1}$ plotted as a function of the oscillator parameter b .

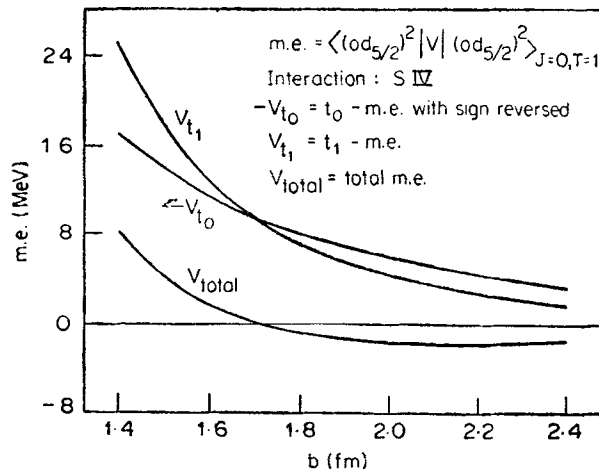


Figure 2. The matrix element $\langle (0 d_{5/2})^2 | V | (0 d_{5/2})^2 \rangle_{J=0, T=1}$ plotted as a function of the oscillator parameter b .

m.e. is therefore positive. After a critical value of b , the t_0 m.e. becomes numerically larger than t_1 m.e. for all values of b and the total m.e. now becomes attractive. In the calculations of nuclear properties, the value of b must be larger than the critical b ($b = 1.7$ fm in this case); otherwise the results would be unphysical. Similar behaviour is exhibited by $(0f_{7/2})^2$ m.e.

The source of this behaviour is the severe b dependence of the m.e. of various parts of the Skyrme force. The t_0 m.e. fall off as b^{-3} while others as b^{-5} except t_3 m.e. which fall off as b^{-6} . There is a competition between the t_0 and t_1 m.e. which leads to the pairing or the antipairing of the m.e. For b value larger than the critical value, the m.e. of t_1 , etc. fall off much faster than t_0 and the total m.e. becomes attractive.

We state that the difficulty raised by Sharp and Zamick can be remedied by optimising b for every nucleus in question. One can then proceed to the calculation of nuclear properties.

3.5. Sensitivity of the calculation on the oscillator parameter

Our calculations do not include configurations beyond the fourth major shell. The truncation of the configuration space makes the HF calculations severely dependent on the oscillator parameter b . If the configuration space is quite large the calculations would be insensitive to the size parameter b . This is particularly true in the case of Skyrme interaction. The saturation would be achieved through the optimisation of b . This value of b is then the proper b to be used in the calculations of spectroscopic properties. For the nuclei studied, the b value ranges from 1.6 fm to 1.9 fm.

3.6. HF properties of nuclei

In this section we shall discuss the results of the HF calculations performed with three variants of Skyrme interaction viz. SII, SIV and SV (table 1). The last variant has $t_3 = 0$ and hence is only a two-body density-independent interaction. In our band-averaged formalism, the former two sets will be denoted by BASII and BASIV respectively. The variant SIV has the weakest density term, while the variant SII has a somewhat larger density dependence. The other two variants viz. SIII and SVI pose the problem of numerical instability of the HF solution and hence that of its convergence through their large density dependence. The corrections arising due to the

Table 1. Parameters of the Skyrme interactions (MeV).

	MeV t_0 fm ³	MeV t_1 fm ⁵	MeV t_2 fm ⁵	MeV t_3 fm ⁶	χ_0	MeV W fm ⁵
SI	-1057.3	235.9	-100.0	14463.5	0.56	120.0
SII	-1169.9	586.6	-27.1	9331.1	0.34	105.0
SIII	-1128.75	395.0	-95.0	14000.0	0.45	120.0
SIV	-1205.6	765.0	35.0	5000.0	0.05	150.0
SV	-1248.29	970.56	107.22	0.0	-0.17	150.0
SVI	-1101.81	271.67	-138.33	17000.0	0.583	115.0

centre-of-mass and Coulomb repulsion have not been included in order to make the projection calculations simpler and also because it was found that contribution of these corrections to the energy spectrum is quite insignificant (Kamblé *et al* 1974).

Table 2. HF properties of nuclei.

Nucleus	Inter-action	b fm	E_{HF} (MeV)	Q_{HF} (fm ²)	RMS fm	Re. En MeV	B.E. (Expt.) MeV	$\epsilon_{0s_{1/2} \pm 1/2}$ MeV	E_{0^+} MeV
⁸ Be	BASII	1.7	- 52.79	63.49	2.6647	-10.44		-28.48	-63.34
	BASIV		- 42.94	47.19	2.5386	-6.44	-56.50	-29.41	-49.18
	SV		- 36.91	44.21	2.5804	—	—	-30.63	-41.32
¹² C	BASII	1.6	- 85.88	-42.80	2.5857	-28.39		-36.27	-93.04
	BASIV		- 81.70	-32.37	2.5583	-15.96	-92.20	-41.23	-87.50
	SV		- 76.22	-32.50	2.5632	—	—	-46.46	-81.18
¹⁶ O	BASIV	1.6	-125.99	0.0	2.6395	-26.36	-127.62	-48.05	—
	SV		-126.68	0.0	2.6322	—	—	-56.36	—
²⁰ Ne	BASII	1.9	-160.63	88.12	2.9301	-58.25	—	-44.57	-165.52
	BASIV		-156.69	74.77	2.9009	-32.64	-160.65	-52.09	-159.77
	SV		-151.52	68.17	2.8835	—	—	-61.24	-153.51
	BASIV-d		-161.18	78.25	2.9068	-32.01	—	-52.72	-168.75

Table 3. HF orbitals for the nucleus ⁸Be with interaction BASIV ($b = 1.7$ fm). The 'range' corresponds to non-zero components of the $s_{1/2}$ deformed orbital with given (m, π) in the total space of 20 basis states ordered with (i) increasing $|m|$, (ii) with decreasing l or j and (iii) with increasing n —the radial quantum number. Only proton time-like orbitals are given. ϵ denotes HF single particle energies. * denotes lowest unoccupied orbital.

Range	m^π	ϵ (MeV)	HF orbitals			
1-4	1/2 ⁺	-29.41	0.176311	-0.183866	0.963942	-0.076962
8-13	1/2 ⁻	-17.44	0.149012	-0.105569	0.838093	-0.145709
14-17*	-3/2 ⁻	- 3.38	0.186543	0.145929	0.960512	-0.146022

Table 4. HF orbitals for the nucleus ¹²C with interaction BASIV ($b = 1.6$ fm). For explanation, see Table 3.

Range	m^π	ϵ (MeV)	HF orbitals			
1-4	1/2 ⁺	-41.23	-0.092928	0.110477	0.988882	-0.035645
14-17	-3/2 ⁻	-20.09	-0.087076	-0.079816	0.981256	-0.152263
8-13	1/2 ⁻	-17.72	-0.096997	-0.033852	0.770395	-0.074295
8-13*	1/2 ⁻	- 4.00	0.106977	-0.104996	-0.603995	0.132727

Table 5. HF orbitals for the nucleus ¹⁶O with interaction BASIV ($b = 1.6$ fm). For explanation, see Table 3.

Range	m^π	ϵ (MeV)	HF orbitals			
1-4	1/2 ⁺	-48.05	0.0	0.0	0.998000	-0.063221
8-13	1/2 ⁻	-23.28	0.0	0.0	0.988050	-0.154137
14-17	-3/2 ⁻	-23.28	0.0	0.0	0.988050	-0.154137
8-13	1/2 ⁻	-15.72	0.0	0.0	0.0	0.0
7-7*	5/2 ⁺	- 1.61	1.0			0.981649

Table 6. HF orbitals for the nucleus ^{20}Ne with interaction BASIV ($b=1.9$ fm)
For explanation, see Table 3.

Range	m^π	$\epsilon(\text{MeV})$	HF orbitals					
1-4	$1/2^+$	-52.09	0.0941056	-0.083123	0.986204	0.107826		
8-13	$1/2^-$	-32.84	0.112374	-0.090761	0.900803	0.067988	-0.403796	-0.003668
14-17	$-3/2^-$	-24.53	0.087974	0.060413	0.988387	0.108174		
8-13	$1/2^-$	-18.23	0.034781	0.092630	0.408981	0.029128	0.905766	0.041083
1-4	$1/2^+$	-12.98	0.859362	-0.280068	-0.059325	-0.423721		
5-6*	$3/2^+$	-8.42	0.976684	0.214682				

In table 2, we display the results of HF calculations with the interactions BASII, BASIV and SV for the nuclei ^8Be , ^{12}C , ^{16}O and ^{20}Ne . We also give the HF orbitals for these nuclei for the variant SIV in tables 3 to 6. It is seen that the variant with stronger density provides a better agreement for the binding energies of these nuclei, but, at the same time it gives a larger deformation of the nucleus. We remark that an interaction having a weak density dependence and reasonable p -wave repulsion would give rise to clustering which will be important for explaining the excited low-lying $4p-4h$ or $8p-8h$ states in nuclei like ^{12}C , ^{16}O and ^{20}Ne .

It should be noted that the interaction BASII and BASIV lift up the deep lying orbitals as compared to SV which is in accordance with the calculations reported by Beiner *et al* (1975). The rms radii given by BASII, however, are seen to be larger than those given by BASIV and SV.

4. HF projected spectra

From the deformed HF solution, good angular momentum states can be projected out employing the standard projection formalism.

4.1. Spectra of ^8Be and ^{12}C

We shall study in this section the projected ground state spectra for the nuclei ^8Be and ^{12}C with the interaction BASII, BASIV and SV obtained from the HF intrinsic solutions. We shall deal with the nucleus ^{20}Ne separately.

In table 2 we have given the HF intrinsic properties of ^{12}C and ^8Be respectively along with the energy of the 0^+ levels in the projected spectrum for the interactions used. For the sake of simplicity and since c.m.m. and coulomb corrections do not affect the spectra significantly, we have not included them in our calculations (Kamble *et al* (1974)).

In figures 3 and 4 we show the projected ground state bands for ^8Be and ^{12}C with BASII, BASIV and SV for the sake of comparison. The 4^+ level obtained with SV for ^{12}C and ^8Be is calculated at a lower energy compared to the experiment. With BASIV, the 4^+ level for ^{12}C gets raised by ~ 1.8 MeV and the 2^+ level is not affected thus giving excellent agreement with experiment. A similar phenomenon is seen in the case of ^8Be . The 4^+ level is raised as much as ~ 2.5 MeV, again giving very good agreement with experiment. It is seen that 2^+ level of ^8Be also gets slightly lifted. BASIV thus provides a much better description than does SV.

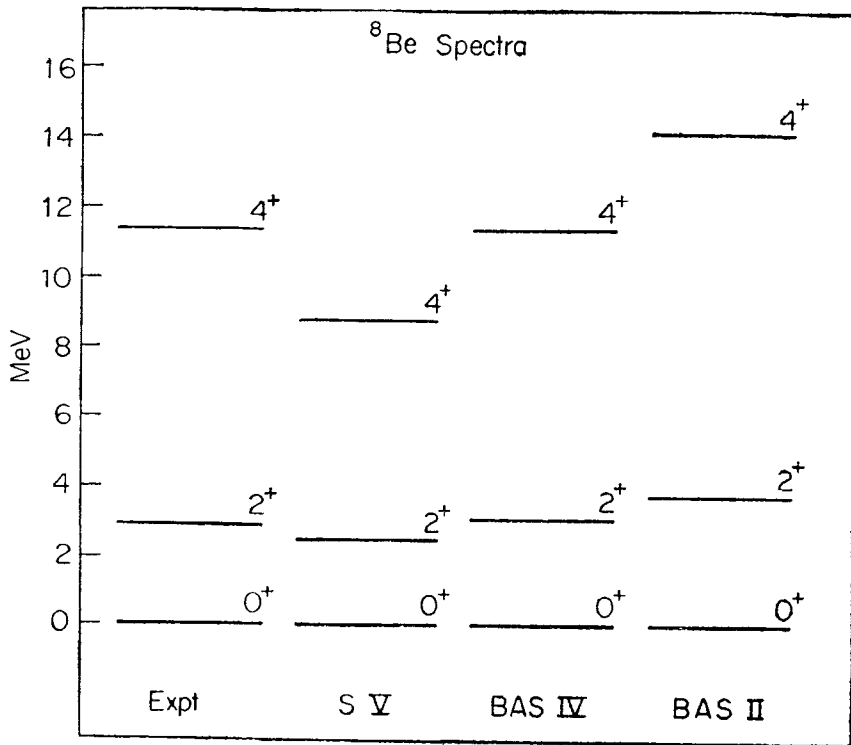


Figure 3. ^8Be spectra calculated with various Skyrme variants.

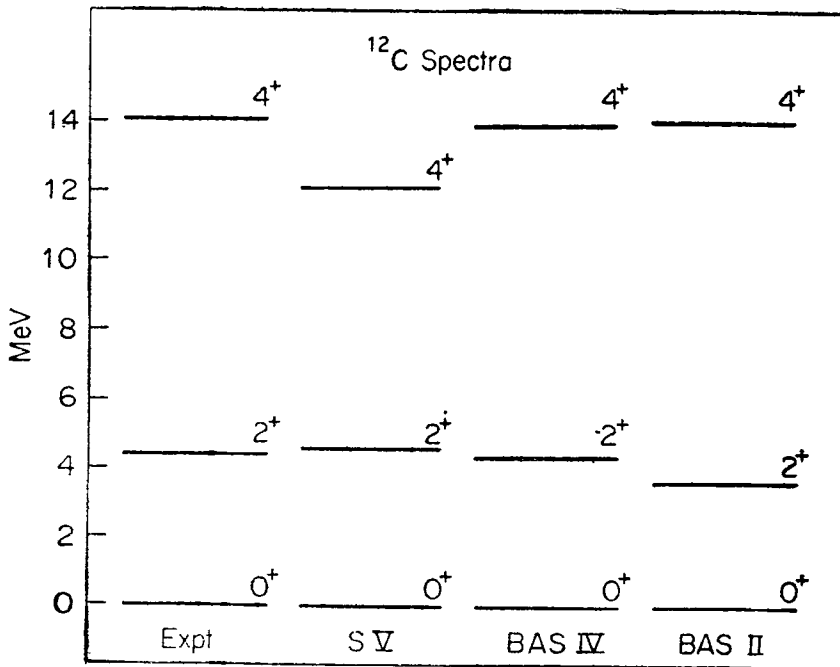


Figure 4. ^{12}C spectra calculated with various Skyrme variants.

The interaction BASII gives a spread out spectrum for ${}^8\text{Be}$. For ${}^{12}\text{C}$, however, it should be remembered that the two-body spin-orbit interaction plays a very important role in explaining the spectrum of ${}^{12}\text{C}$ (Kamble and Khadkikar 1975). The variant SII has a weak spin-orbit force ($W = 120 \text{ MeV fm}^5$ as compared to $W = 150 \text{ MeV fm}^5$ for SIV and SV). Hence one would expect a somewhat compressed spectrum for ${}^{12}\text{C}$ compared to BASIV and SV. The fact that BASII, a variant with a stronger density, gives a spectrum which is more or less the same as given by the previous variants again shows the tendency of BASII to spread out the spectra as in the case of ${}^8\text{Be}$. From these spectra, one can infer that the Skyrme variants with stronger densities would give rise to more spread-out spectra. We see that the introduction of density dependence dramatically raises the higher angular momentum states in both the nuclei providing excellent agreement with experiment.

4.2. Spectra of ${}^{20}\text{Ne}$

In this section we shall study the projected spectra of ${}^{20}\text{Ne}$. Passler and Mosel (1976) have performed the calculations for this nucleus in the self-consistent cranking model (CHF) using the various Skyrme variants available in the configuration space of first five major shells. It has been, however, shown (Sharma *et al* 1976) that CHF approximation is only a prescription to obtain the approximate behaviour of the rotational spectrum. Although the deformed density makes the Skyrme force unsuitable for rigorous spectroscopic calculations requiring good angular momentum states, Passler and Mosel use this force to calculate the rotational spectrum of ${}^{20}\text{Ne}$. They obtain too compressed spectra with all conventional Skyrme variants. Therefore they adjust the p -state part of the interaction (the strength parameter t_2) and the s -state repulsive part (the strength parameter t_1) keeping all other parameters constant in such a way that the rotational spectrum of ${}^{20}\text{Ne}$ is obtained satisfactorily without modifying the calculated ground state energy. They obtain a reasonably good agreement for ${}^{20}\text{Ne}$ rotational spectrum with the variant SIV- d in which $t_1 = 530 \text{ MeV fm}^5$ and $t_2 = 309.3 \text{ MeV fm}^5$ compared to $t_1 = 765 \text{ MeV fm}^5$ and $t_2 = 35 \text{ MeV fm}^5$ in SIV with other parameters constant.

Passler and Mosel attributed the reasons for large moments of inertia and hence compressed spectra to the small p -state repulsive part (t_2) and the s -state repulsive part (t_1) of the variant SIV of the Skyrme force. They therefore increased t_2 and decreased t_1 in SIV to obtain the variant SIV- d . They obtained larger gaps with SIV- d which agrees with our results also.

We show in table 2 the HF intrinsic properties obtained for ${}^{20}\text{Ne}$ with SV, BASII, BASIV and BASIV- d interactions along with the energy of the 0^+ state of the ground state band. The results of our calculations for the rotational spectra of ${}^{20}\text{Ne}$ with BASIV, BASIV- d and SV are displayed in figure 5. It is seen that the variant SV gives compressed spectra in both PHF as well as CHF formalisms. It is to be noted that the interaction BASIV gives good agreement in our projected HF calculation, while CHF gives a compressed spectrum. The variant SIV- d which provides a good agreement with CHF gives a highly spread-out spectrum in PHF formalism. In either case, the PHF spectrum is quite spread out compared with the CHF spectrum. It can be seen that BASII gives much more spread-out spectra as in the case of ${}^8\text{Be}$.

It should be remarked that the CHF procedure involves a transformation to the

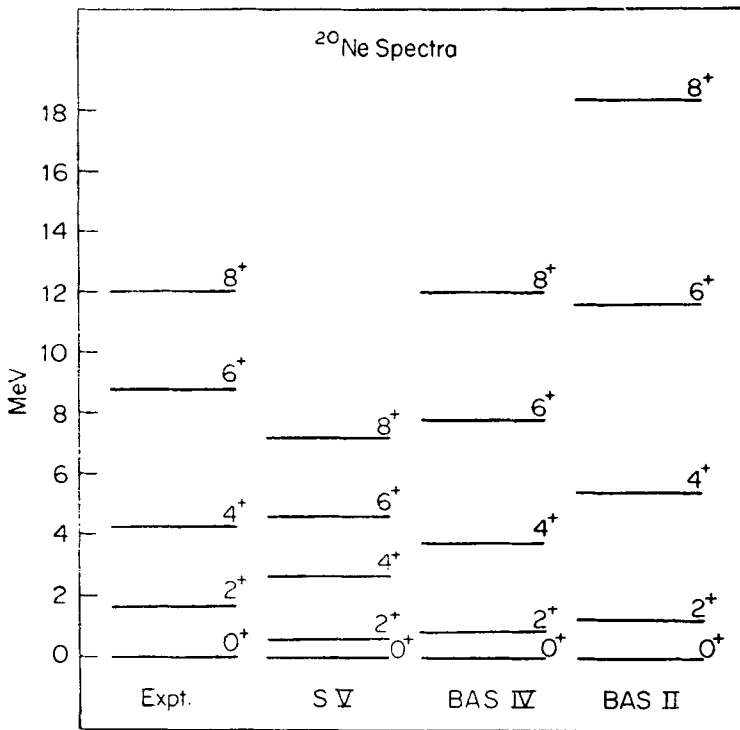


Figure 5. ²⁰Ne spectra calculated with various Skyrme variants.

uniformly rotating frame of reference and so implies semi-classical, semi-adiabatic approximation. For a band with finite cut-off for angular momentum, this approximation would be valid for angular velocity $\omega \ll \omega_{\text{cut-off}}$ and at the same time $\langle J^2 \rangle$ should be sufficiently large so that the quantum fluctuations across the rotation axis are small. This implies that the moment of inertia I should be large which is corroborated by the actual comparison of the spectrum.

The spectra of $4-n$ type nuclei calculated by Caurier and Grammaticos (1977) in LS coupling using three-body version of Skyrme force also are quite compressed. The spectra of such nuclei calculated in our model of band-averaged density are, however, spread out. The introduction of density dependence in Skyrme interaction spreads out the energy spectra. This opposite trend could be due to the following factors. It should be noted that the spin-orbit force has not been included in the calculations reported by Caurier and Grammaticos, while it has been shown by us (Kamble and Khadkikar 1975) that the two-body spin-orbit force is extremely important for explaining the spectrum of ¹²C. Also the configuration space of first four major shells used by us may need to be expanded to incorporate higher single-particle configurations. It also should be remembered that the three-body contact and two-body density-dependent versions of the Skyrme interaction are equivalent only for the HF calculations of bulk properties of even-even time reversal invariant nuclei and hence may give rise to different spectroscopic properties.

We thus find that BASIV provides a better description than SV or BASII. We see that the SIV is one Skyrme variant which provides simultaneous agreement for

both bulk as well as spectroscopic properties of these nuclei. It would be quite interesting to check this point by extending these calculations to other nuclei in this region as well as heavier nuclei. This programme is being pursued.

4.3. Individual contributions of various parts of Skyrme interaction to nuclear spectra

We saw in the preceding sections that Skyrme force provides a reasonably good agreement to the bulk properties of the even-even nuclei as well as the ground state energy spectra for ${}^8\text{Be}$, ${}^{12}\text{C}$ and ${}^{20}\text{Ne}$. In the case of ${}^{12}\text{C}$ it was shown that the two-body spin-orbit force (W) was crucial in explaining the energy spectrum. It has been shown in earlier calculations that the p -state interaction term (t_2) and the three-body contact interaction term (t_3) simulating a two-body density-dependent interaction affect clustering in alpha cluster model. It is therefore quite interesting to study the individual contributions of all the terms in the Skyrme interaction to the energy spectra of nuclei. In the following we shall present the calculations for the individual contributions of various parts of Skyrme interaction to the spectra of the nuclei we have studied so far. We shall see that most of the contribution to the energy spectra comes from the s -state attractive (t_0) and the s -state repulsive (t_1) parts of the Skyrme interaction apart from that due to kinetic energy.

In table 7 we give the individual contributions of all the terms of the Skyrme interaction for the ground state $K = 0$ bands for ${}^8\text{Be}$, ${}^{12}\text{C}$ and ${}^{20}\text{Ne}$ calculated with the interaction BASIV. One can see from the table that most of the contribution to any J state comes from the s -state attractive (t_0) and s -state repulsive (t_1) parts of the Skyrme interaction. The effect of other terms is quite small. The spin-orbit term (W) however contributes significantly to the spectrum in the case of ${}^{12}\text{C}$ similar to the results obtained using the variant SV. It can be seen that the effect of the terms t_0 and W is to spread out the spectrum while that of t_1 , t_2 and t_3 is to compress it. The individual contribution to energy spacing of these terms is roughly proportional to their individual contributions to the binding energies. The parameters t_2 and t_3 are rather small in the variant SIV and hence such calculations with other Skyrme vari-

Table 7. Individual contribution of various parts of Skyrme interaction to the energy spectra (Interaction BASIV). All contributions in MeV.

Nucleus	J	K_E	t_0	t_1	t_2	W	t_3	Total
${}^8\text{Be}$	0	111.02	-285.16	113.27	0.97	-2.55	13.28	-49.18
	2	112.33	-279.76	109.74	0.95	-2.37	13.00	-46.12
	4	116.84	-268.86	103.03	0.90	-2.05	12.32	-37.81
${}^{12}\text{C}$	0	183.59	-470.00	176.96	4.42	-14.51	32.67	-87.50
	2	183.85	-464.30	171.96	4.27	-11.34	32.37	-83.20
	4	186.69	-450.51	162.94	4.06	-7.90	31.12	-73.60
${}^{20}\text{Ne}$	0	313.69	-835.06	294.93	11.09	-10.13	65.71	-159.77
	2	313.85	-831.62	291.95	11.08	-9.86	65.65	-158.95
	4	314.74	-825.26	287.39	11.01	-9.31	65.34	-156.09
	6	315.96	-814.13	279.28	10.92	-8.68	64.64	-152.02
	8	317.35	-807.68	276.06	10.83	-8.39	64.04	-147.79

ants would be quite instructive to have an insight into the spectroscopic calculations with Skyrme interaction. In the present calculation, however, we see that the s -state attractive (t_0) and s -state repulsive (t_1) parts of the Skyrme interaction are the dominant terms which decide the overall nature of the spectrum.

The effect of terms t_2 and t_3 is to change the nature such as the deformation of the intrinsic states and is indirect as far as the spectrum is concerned. However, the strength of the s -state repulsion is governed by the strength of the p -state repulsion and that of the density dependence to obtain overall agreement for the bulk properties and thus contributes in deciding the nature of the spectrum.

5. Electromagnetic properties

In table 8 we have listed the electric quadrupole and magnetic dipole moments in the projected $J = 2^+$ state for the nuclei studied. Unfortunately, the experimental data available at present are extremely scanty. In the case of ^{20}Ne , the experimental value of Q is not satisfactorily reproduced by any of the Skyrme variants used. It is however seen that the interaction BASII gives a value which is closest to the experimental value. More data on these properties are highly desirable, so as to compare the theoretical predictions. In table 9, we display the reduced transition rates $B(E2)$ for these nuclei. No data are possible for ^8Be . In the case of ^{12}C , both SV and BASIV reproduce the $B(E2)$ values quite well. For ^{20}Ne , the $B(E2)$ data available indicate that the trend of experimental transition rates cannot be reproduced by any of the variants used. The transition rates calculated with the Sussex interaction (Elliott *et al* 1968) and in the framework of shell model (Halbert *et al* 1971) are also shown for comparison. Although the two $B(E2, 2 \rightarrow 0)$ estimates show a large amount of error in the experimental determination of this quantity, the trends obtained with shell model and with the interactions which are independent of density such as Sussex and SV for the transitions shown are exactly opposite to the experimental one. On the other hand, with the introduction of density dependence, though the experimental trend is not reproduced, the successive $B(E2)$ rates seem to increase as can be seen from table 9 for the transitions $2 \rightarrow 0$, $4 \rightarrow 2$ and $6 \rightarrow 4$. BASIV seems to give a

Table 8. Electromagnetic properties of nuclei.

Nucleus	Interaction	$Q_{J=2^+}$ $e \text{ fm}^2$	$\mu_{J=2^+}$ n m
^8Be	BASII	-9.8367	0.8008
	BASIV	-7.6838	0.7111
	SV	-7.5755	0.7927
^{12}C	BASII	6.8063	0.7851
	BASIV	5.9048	0.7718
	SV	5.4942	0.7297
^{20}Ne	BASII	-14.0382	1.0547
	BASIV	-12.0641	1.0732
	SV	-11.1104	1.0813
	EXPT.	-24.0 ± 3.0	

Table 9. Reduced transition rates $B(E2, J_i \rightarrow J_f)$ for the nuclei ${}^8\text{Be}$, ${}^{12}\text{C}$ and ${}^{20}\text{Ne}$.

Nucleus	Transition		Interaction	$B(E2, J_i \rightarrow J_f)$		
	J_i	J_f		Cal $e^2 \text{fm}^4$	Expt $e^2 \text{fm}^4$	
${}^8\text{Be}$	2	0	BASII	115.92		
			BASIV	70.35		
			SV	67.99		
	2	0	BASII	12.05		8.46 ± 0.60
			BASIV	9.38		
			SV	7.96		
${}^{12}\text{C}$	4	2	BASII	18.64		
			BASIV	14.69		
			SV	11.87		
	6	4	BASII	20.77		—
			BASIV	16.96		
			SV	14.49		
${}^{20}\text{Ne}$	2	0	BASII	47.62	57 ± 8	
			BASIV	35.37		
			SV	30.08		
			SUSSEX	22.45		
			SHELL MODEL	48.10		
	4	2	BASII	63.98	49.7 ± 4.5	
			BASIV	47.61		
			SV	40.19		
			SUSSEX	30.16		
			SHELL MODEL	59.70		
6	4	BASII	70.69	89.8 ± 19.2		
		BASIV	48.08			
		SV	38.31			
		SUSSEX	26.44			
		SHELL MODEL	48.80			

better agreement for $B(E2, 4 \rightarrow 2)$ which appears to be most reliable, whereas BASII gives a better agreement for $B(E2, 6 \rightarrow 4)$. The results may be improved by expanding the configuration space to include higher single particle states. Better experimental determination of these transition rates is therefore highly desirable.

6. Conclusions

In this paper we have defined a modification in the Skyrme interaction so that the deformed density is replaced by the scalar band averaged density rendering the spectroscopic calculations completely feasible. We have shown that the introduction of density dependence spreads out the energy spectra and gives better agreement with the binding energies, although the Skyrme variants with larger density dependence give rise to HF solutions with larger deformations.

It is seen that the Skyrme variant SIV which has a weak density dependence gives best overall agreement for energy spectra and the available data for the electromagnetic properties of the nuclei studied. Other Skyrme variants with strong density dependence (SIII and SVI) are expected to give even more spread-out spectra than

does SII. Hence it appears that the Skyrme variant SIV is the one which offers simultaneous agreement for bulk as well as spectroscopic properties of the light nuclei such as ^8Be , ^{12}C and ^{20}Ne .

It is also seen that the most contribution to nuclear spectra for any angular momentum state comes from the s -state attractive and s -state repulsive parts of the Skyrme interaction.

It can be seen from the parameters of the Skyrme variants SII to SVI that the surface thickness parameter ($9t_1 - 5t_2$) gradually decreases as the density dependence of the interaction increases. This would affect the binding energies especially of the light deformed nuclei. One can see that a smaller value of this parameter consistently gives rise to better binding. It may be remarked that a larger surface thickness would prefer more alpha-clustering. Thus among the variants SII to SVI, SV and SVI would give rise to maximum and minimum alpha-clustering. The parameter ($3t_1 + 5t_2$) is responsible for the level densities of the HF single particle energies. It is known that the stronger density dependence gives rise to more compressed single particle spectra. Because of this effect one expects that stronger density dependence would give rise to more deformed HF solutions. This is seen to be the case in the present calculations. Finally, the calculations need to be extended to other heavier nuclei and include pairing correlations in order to study high-spin states and other phenomena like back-bending. Such calculations are in progress and would be reported elsewhere.

References

- Beiner M, Flocard H, Nguen van Giai and Quentin P 1975 *Nucl. Phys.* **A238** 29
 Bell J S and Skyrme T H R 1956 *Philos. Mag.* **1** 1055
 Bertsch G F and Tsai S F 1975 *Phys. Rep.* **18** 125
 Caurier E and Grammaticos B 1977 *Nucl. Phys.* **A279** 333
 Chang B D 1975 *Phys. Lett.* **B56** 205
 Elliott J P, Jackson A D, Mavromatis H A, Sanderson E A and Singh B 1968 *Nucl. Phys.* **A121** 241
 Friar J L and Negele J W 1975 *Nucl. Phys.* **A240** 301
 Kamble V B, Khadkikar S B and Kulkarni D R 1974 *Proc. Nucl. Phys. Solid State Phys. Symp., Bombay* **B17** 204
 Kamble V B and Khadkikar S B 1975 *Phys. Lett.* **B59** 19
 Khadkikar S B and Kamble V B 1974 *Nucl. Phys.* **A225** 352
 Khadkikar S B and Kamble V B 1976 *Phys. Lett.* **B64** 131
 Koopmans T 1934 *Physica* **1** 104
 Halbert E C, McGrory J B, Wildenthal B H and Pandya S P 1971 *Adv. Nucl. Phys.* **4** 315
 Passler K H 1976 *Nucl. Phys.* **A257** 253
 Passler K H and Mosel U 1976 *Nucl. Phys.* **A257** 242
 Ripka G 1969 14th International meeting on fast neutrons and the study of nuclear structure, Yugoslavia
 Sharma S K, Satpathy L, Khadkikar S B and Nair S C K 1976 *Phys. Lett.* **B61** 122
 Sharp R W and Zamick L 1973 *Nucl. Phys.* **A208** 130
 Skyrme T H R 1956 *Philos. Mag.* **1** 1043
 Skyrme T H R 1959 *Nucl. Phys.* **9** 615
 Vautherin D and Brink D M 1972 *Phys. Rev.* **C5** 626
 Vautherin D 1973 *Phys. Rev.* **C7** 296
 Zofka J and Ripka G 1971 *Nucl. Phys.* **A168** 65